



**HAL**  
open science

## Sharp estimates for the integrated density of states in Anderson tight-binding models

Perceval Desforges, Svitlana Mayboroda, Shiwen Zhang, Guy David, Douglas  
Arnold, Wei Wang, Marcel Filoche

► **To cite this version:**

Perceval Desforges, Svitlana Mayboroda, Shiwen Zhang, Guy David, Douglas Arnold, et al.. Sharp estimates for the integrated density of states in Anderson tight-binding models. *Physical Review A*, 2021, 104 (1), 10.1103/PhysRevA.104.012207 . hal-03285506

**HAL Id: hal-03285506**

**<https://hal.science/hal-03285506>**

Submitted on 13 Jul 2021

**HAL** is a multi-disciplinary open access archive for the deposit and dissemination of scientific research documents, whether they are published or not. The documents may come from teaching and research institutions in France or abroad, or from public or private research centers.

L'archive ouverte pluridisciplinaire **HAL**, est destinée au dépôt et à la diffusion de documents scientifiques de niveau recherche, publiés ou non, émanant des établissements d'enseignement et de recherche français ou étrangers, des laboratoires publics ou privés.

# Sharp estimates for the integrated density of states in Anderson tight-binding models

Perceval Desforges,<sup>1</sup> Svitlana Mayboroda,<sup>2</sup> Shiwen Zhang,<sup>2</sup> Guy David,<sup>3</sup> Douglas N. Arnold,<sup>2</sup> Wei Wang,<sup>2</sup> and Marcel Filoche<sup>1</sup>

<sup>1</sup>*Laboratoire de Physique de la Matière Condensée,*

*Ecole Polytechnique, CNRS, IP Paris, Palaiseau F-91128, France*

<sup>2</sup>*School of Mathematics, University of Minnesota, Minneapolis, Minnesota 55455, USA*

<sup>3</sup>*Université Paris-Saclay, Laboratoire de Mathématiques, CNRS, UMR F-91405 Orsay, France*

(Dated: October 20, 2020)

Recent work [1] has proved the existence of bounds from above and below for the Integrated Density of States (IDOS) of the Schrödinger operator throughout the spectrum, called the *Landscape Law*. These bounds involve dimensional constants whose optimal values are yet to be determined. Here, we investigate the accuracy of the Landscape Law in 1D and 2D tight-binding Anderson models, with binary or uniform random distributions. We show, in particular, that in 1D, the IDOS can be approximated with high accuracy through a single formula involving a remarkably simple multiplicative energy shift. In 2D, the same idea applies but the prefactor has to be changed between the bottom and top parts of the spectrum.

In single-particle quantum systems subject to random potential, the Integrated Density of States (IDOS, or counting function, denoted hereafter as  $N(E)$ ) departs significantly at low energy from the high energy asymptotic behavior known as Weyl's formula. According to it, in the absence of any potential,  $N(E)$  scales as  $E^{d/2}$  where  $d$  is the ambient dimension. However, in the presence of a disordered or random potential the IDOS exhibits a very slowly growing tail at low energy. In 1964, Lifshitz proposed a model where the integrated density of states would drop off exponentially as  $E$  approaches its minimum value  $E_0$ , forming what is known as a *Lifshitz tail* [2, 3]:

$$N(E) \sim C \exp\left(-c(E - E_0)^{-\frac{d}{2}}\right). \quad (1)$$

Since then, understanding the precise behavior of the density of states in the presence of disorder has been the subject of a very rich literature (for an extended review on the topic, the reader can refer to [4–6]). The existence of Lifshitz tails for the Poisson random potential was proved in [7–10]. Later Kirsch and Martinelli gave a proof close to Lifshitz's intuition for a large class of random potentials in the continuous setting in [11], while Simon generalized the argument to the tight binding model [12]. However, the only mathematical statement that could be rigorously proven in full generality had not the shape of Eq. (1) but the weaker form:

$$\lim_{E \rightarrow E_0} \frac{\ln(|\ln(N(E))|)}{\ln(E - E_0)} = -\frac{d}{2}. \quad (2)$$

These results are asymptotic in the limit of vanishing  $E - E_0$ . For the tight-binding model, for particular cases of uniform or binary potential, better results are known [6, 12–14] but they do not apply to all probability laws. Away from the asymptotic behavior at low energy, Klopp and Elgart showed that in the weak disorder limit these Lifshitz tails extend roughly up to the average of the potential [15–17]. To this day, many unsolved questions remain concerning these Lifshitz tails: (i) Can one

improve the known result by deriving a general estimate on  $\ln(N(E))$  and not on  $\ln(|\ln(N(E))|)$ ? (ii) How does disorder enter the estimate? More precisely, can one generalize existing results showing logarithmic corrections for random uniform disorder as compared to binary disorder [18, 19]? (iii) Can these results be extended to a full interval instead of being asymptotic near the lower bound of the spectrum?

In this article, we present a new function, denoted  $N_u(E)$  and called *Landscape Law* [1], that provides the first estimates from above and below to the actual counting function throughout the spectrum. This function is obtained from the *localization landscape*, a theoretical tool introduced in 2012 and developed in the recent years [20, 21]. Not only do these estimates cover the entire range of energy for any type of potential or disorder, but they also provide the asymptotic behavior of  $\ln(N(E))$  at low energy for random uniform or binary disorder, thus removing a log from the previously known results. In particular, we obtain the logarithmic correction in the case of the uniform Anderson model. We investigate numerically the optimal constants involved in the bounds, and observe their similarity for both aforementioned types of disorder. Finally, we test whether these mathematically proven bounds from above and below could in fact be merged into one single approximate formula based on  $N_u$ , thus providing a very fast and efficient way of predicting the behavior IDOS on the entire spectrum even in a random or complicated system.

We consider a  $d$ -dimensional tight-binding model. The corresponding Hamiltonian is

$$\hat{H} = \sum_i V_i a_i^\dagger a_i - t \sum_{\langle i,j \rangle} \left( a_i^\dagger a_j + h.c. \right), \quad (3)$$

where  $\langle i,j \rangle$  denotes the sum over nearest neighbors,  $t$  is the hopping term,  $V_i$  is the on-site random potential (on a grid of lattice parameter 1), and  $a_i^\dagger$  and  $a_i$  are the creation and annihilation operators, respectively. The  $V_i$  are i.i.d. variables and follow a random law which can be

either uniform or binary in our study. The localization landscape  $u$  in this system is defined as the solution to  $\hat{H}u = 1$ , the right-hand side being the constant vector. It has been shown in [22] that the function  $W \equiv 1/u$  defines an effective potential for all quantum states in the tight-binding model, and that this potential provides a remarkably accurate estimate of the energy of the lower-energy states.

Using this effective potential, the function  $N_u(E)$  is defined as follows: for a given energy  $E$ , we partition the entire domain into  $d$ -cubes (intervals in 1D, squares in 2D, ...) of sidelength  $E^{-1/2}$ .  $N_u(E)$  is then defined as the fraction of cubes for which the minimum of  $W$  over the cube is smaller than  $E$ :

$$N_u(E) \equiv \frac{1}{|\Omega|} \times \left( \begin{array}{l} \text{number of cubes of size } \frac{1}{\sqrt{E}} \\ \text{where } \min(W) \leq E \end{array} \right) \quad (4)$$

For the continuous model, it has been mathematically proven in [1] that there exist constants  $C_4, C_5, C_6$  such that  $N_u$  satisfies the following inequalities:

$$C_5 N_u(C_6 E) \leq N(E) \leq N_u(C_4 E), \quad (5)$$

where  $N(E)$  is the *normalized* IDOS (i.e., the IDOS per unit volume; we will keep this notation for the rest of the article), where the constants  $C_5$  and  $C_6$  depend only on the dimension  $d$  and on the average of the potential, and  $C_4$  depends only on the dimension. When the potential is random, this inequality is verified for the expectations of the IDOS (note that these expectations become deterministic quantities in an infinite domain). To our knowledge, these inequalities are the first universal bounds for the counting function  $N(E)$  of a Schrödinger Hamiltonian throughout the entire spectrum. In other words, unlike Weyl's formula or Lifshitz tails, they are not asymptotic. The proof is rather technical and is based on the analysis of the low values of effective potential  $W$ . A sketch of the proof is given in Supplementary Material. We are currently preparing a version of this proof for discrete tight-binding models.

An example of the sharpness and the predictive power of this inequality is provided in Fig. 1 which displays the actual IDOS  $N(E)$  (blue) and the landscape law  $N_u(E)$  (red) for one realization of a random i.i.d. binary disorder with periodic boundary conditions. The potential can take the values either 0 or  $V_{\max} = 1$  with equal probability on each site of a one-dimensional domain of  $N = 10^5$  sites.  $N(E)$  is computed using the  $LDL^T$  factorization and Sylvester's law of inertia [23]. One can see how the two curves, plotted on a log-log scale, follow each other very closely. On this log-log plot, the upper and lower bounds of (5) would correspond simply to horizontal and vertical translations of the graph of  $N_u(E)$ .

While Ref. [1] proves the existence of the constants  $C_4, C_5, C_6$ , it does not bring any insight on their sharpest values. Indeed, strictly speaking, [1] gives a "tube" containing the IDOS (in log-log plot), and while it is remarkable

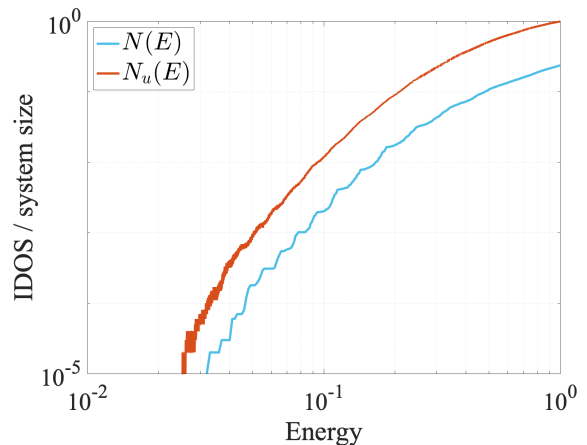


FIG. 1. Counting function  $N(E)$  (blue) and landscape law  $N_u(E)$  (red) for one realization of a one-dimensional binary Anderson tight-binding model. The number of sites is  $N = 10^5$  and the values of the on-site potential are either 0 or 1.

that the tube diameter does not depend on the energy, it could be quite wide if the constants are very different. The goal of this study is threefold: first, to demonstrate the accuracy of the Landscape Law in approximating the actual IDOS. Second, to determine numerically the sharpest values for the constants entering the bounds in (5). This is of particular relevance for  $C_4$  which is predicted to be universal, i.e., to depend only on the dimension  $d$  and not on the particular potential. Third, to assess the possibility to provide an optimal approximation to the IDOS  $N(E)$  (rather than a tube), i.e., for instance a constant  $C_{5,\text{fit}}$  such that  $N(E) \approx C_{5,\text{fit}} N_u(C_6 E)$ .

One starts with the same system as in Fig. 1, but this time  $N(E)$  is averaged over 1000 realizations. Figure 2a displays the corresponding  $N(E)$  and  $N_u(E)$ . In order to determine the constants  $C_4, C_5, C_6$ , we first restrict our study to the domain  $E > 0.02$  to avoid the noise at very low energy. We observe that the graph of  $N_u(E)$  is always above the graph of  $N(E)$ , which means that  $C_4 < 1$ . The value of the constant  $C_4$  corresponds in log-log scale to the largest possible right-shift of the graph of  $N_u$  (or in other words to the smallest possible value of  $C$ ) such that  $N(E) \leq N_u(CE)$ . Here, this value is found to be  $C_4 \approx 0.79$  (or  $1/C_4 \approx 1.26$ ). To find the values of  $C_5$  and  $C_6$ , we first look for the optimal value  $C$  such that  $N(E)/N_u(CE)$  is as constant as possible. This is achieved by taking the minimum of the standard deviation of  $\ln(N(E)/N_u(CE))$  when varying  $C$ . Figure 2b displays this standard deviation for values of  $C$  ranging from 0.5 to 1. One observe a clear minimum at  $C_6 \approx 0.90$  (or  $1/C_6 \approx 1.11$ ). Finally the minimum of the graph of  $N(E)/N_u(C_6 E)$  provides us the sharpest value of  $C_5$  (see Fig. 2c): it is here  $C_5 \approx 0.18$ . However, one can observe that if we were looking for a best fit for  $C_5$  (instead of a lower bound for (5)), then the best fit would be closer to  $C_{5,\text{fit}} \approx 1/4.08$  (obtained by computing the average of  $\ln(N(E)/N_u(C_6 E))$  for  $E > 0.02$ ). With these constants,

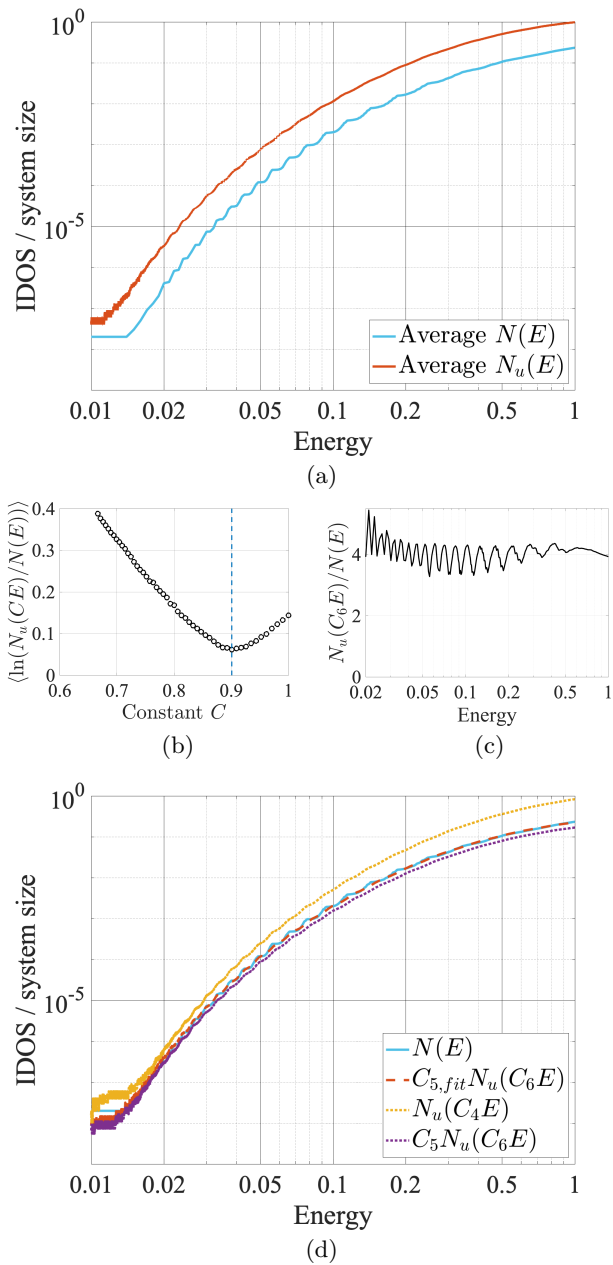


FIG. 2. (a)  $N(E)$  (blue) averaged over 1000 random realizations, and averaged landscape law  $N_u(E)$  (red), for a one-dimensional binary Anderson tight-binding model of size  $N = 10^5$  and  $V_{\max} = 1$ . (b) Standard deviation of the distribution of values of  $\ln(N_u(CE)/N(E))$  for various values of  $C$ . The minimum around  $C = 0.90 \approx 1/1.11$  provides the value of  $C_6$ . (c) Plot of  $N_u(C_6E)/N(E)$ . The maximum shows that one can take  $C_5 = 1/5.45$ . A best fit for  $N(E)$  is obtained by taking the average value  $C_{5,\text{fit}} \approx 1/4.08$ . (d) Final comparison between the original  $N(E)$  (blue), the best fit  $C_{5,\text{fit}} N_u(C_6E)$  (red), and the two bounds from above of below in Eq. (5)  $N_u(C_4E)$  and  $C_5 N_u(C_6E)$  (dotted lines). Note that the best fit is so close to the actual IDOS that the blue line is almost invisible.

the agreement between the actual IDOS and the rescaled

formula based on the localization landscape is excellent throughout the computed spectrum (see Fig. 2d). This means that the inequalities in (4) can almost be transformed into an equality:

$$N(E) \approx C_{5,\text{fit}} N_u(C_6E) \quad (6)$$

The same methodology is then applied to one-dimensional uniform Anderson tight binding model ( $N = 10^5$ ), and to two-dimensional binary and uniform Anderson tight binding models. Figure 3 displays the results for a uniform Anderson model of disorder amplitude  $V_{\max} = 1$ . Here also, we observe that the landscape law  $N_u(E)$  follows very closely the actual IDOS  $N(E)$ . After computation, the value found for  $C_4$  in this case is  $C_4 \approx 0.78 = 1/1.28$ . Further analysis of the standard deviation of the values of  $N_u(CE)/N(E)$  as a function of  $C$  (see Fig. 3b) yields  $C_6 \approx 0.84 = 1/1.19$ . Plotting now  $N_u(C_6E)/N(E)$  as a function of  $E$  (Fig. 3c), one observes that it oscillates slowly between 3 and 5 in the noiseless part of the graph. A possible choice for  $C_5$  is then  $C_5 = 1/4.85$ , but the best fit is obtained for  $C_{5,\text{fit}} = 1/3.94$ , as confirmed in Fig. 3d.

In order to check the validity of our approach, we have investigated the role of the domain size for these one-dimensional Hamiltonians (we could not run such a study in 2D because the computation time did not allow us to explore a large enough range of domain sizes). Domain sizes  $N = 10^3$ ,  $10^4$ , and  $10^5$  are simulated, for both Anderson binary and Anderson uniform models. As expected, the values of the constants  $C_4$ ,  $C_5$ ,  $C_{5,\text{fit}}$ , and  $C_6$  do not seem to depend at all on the domain size (see Table I).

Changing the disorder amplitude does not seem to affect the quality of the approximation either. For instance, Fig. 4 displays the analysis of the Anderson uniform model for  $V_{\max} = 4$ . Once again, one can observe that the fit is excellent throughout the spectrum, justifying again Eq. (6).

Let us now turn to the study of two-dimensional systems. The considered domain is a square of sidelength  $L = 1500$  which corresponds to  $N = 2.25 \times 10^6$  sites. Given that the system size is more than 10 times the size of the studied one-dimensional systems, we could average only over 100 realizations for computational reasons. The fact that the sidelength of the system has been reduced by three orders of magnitude when going from 1D to 2D shifted considerably the lower bound of the energy range that could be explored. In the following simulations, we were unable to go below  $E_{\min} \approx 0.2$ .

Figure 5 displays the analysis for a 2D binary Anderson model. The constants extracted from the analysis are  $C_4 = 1/1.53$ ,  $C_{5,\text{fit}} = 1/14.5$ ,  $C_6 = 1/1.42$ . The agreement between  $N(E)$  and the rescaled landscape law is still good in the whole energy range, even though one can see now that the ratio  $N_u(C_6E)/N(E)$  oscillates much more than in the one-dimensional case. This observation is even more marked in the case of the 2D uniform Anderson case (see Fig. 6). In this last situation, we chose

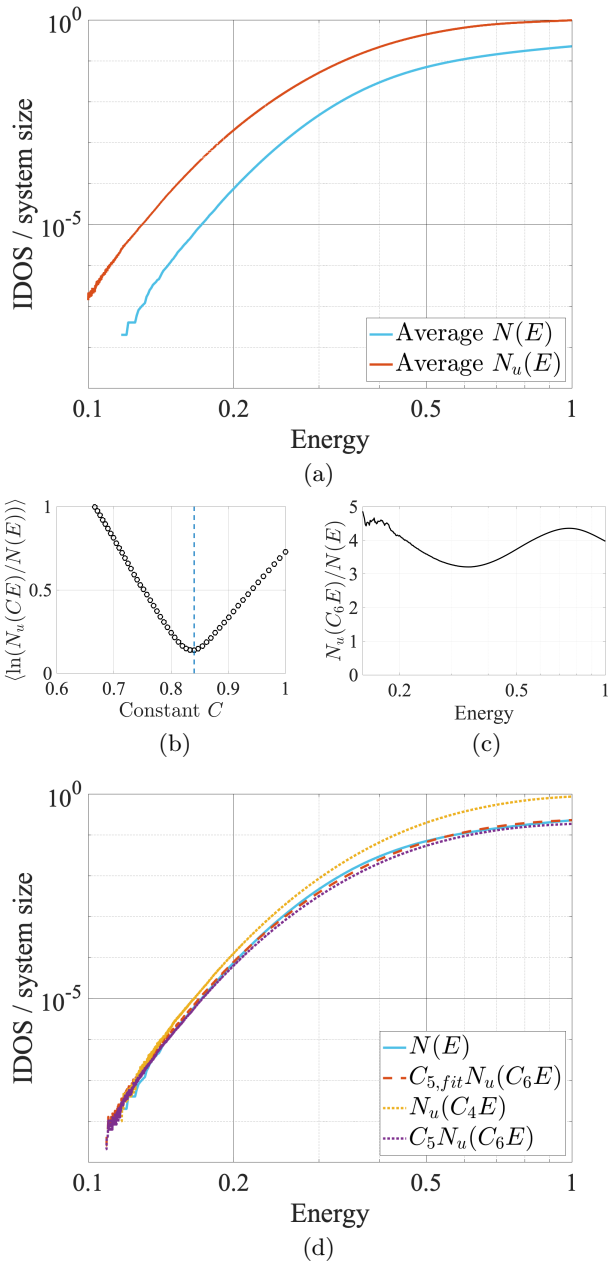


FIG. 3. (a)  $N(E)$  (blue) averaged over 1000 random realizations, and averaged landscape law  $N_u(E)$  (red), for a one-dimensional uniform Anderson tight-binding model of size  $N = 10^5$  and  $V_{\max} = 1$ . (b) Standard deviation of the distribution of values of  $\ln(N_u(CE)/N(E))$  for various values of  $C$ . The minimum around  $C = 0.84 \approx 1/1.19$  provides the value of  $C_6$ . (c) Plot of  $N_u(C_6 E)/N(E)$ . The maximum shows that one can take  $C_5 = 1/4.85$ . A best fit for  $N(E)$  is obtained by taking the average value  $C_{5,\text{fit}} \approx 1/3.94$ . (d) Final comparison between the original  $N(E)$ , the best fit  $C_{5,\text{fit}} N_u(C_6 E)$ , and the two bounds from above of below  $N_u(C_4 E)$  and  $C_5 N_u(C_6 E)$  (dotted lines).

to display not only the best fit (in green), but also the upper and lower bounds to  $N(E)$  obtained by rescaling  $N_u(E)$ . One can see that they are significantly apart,

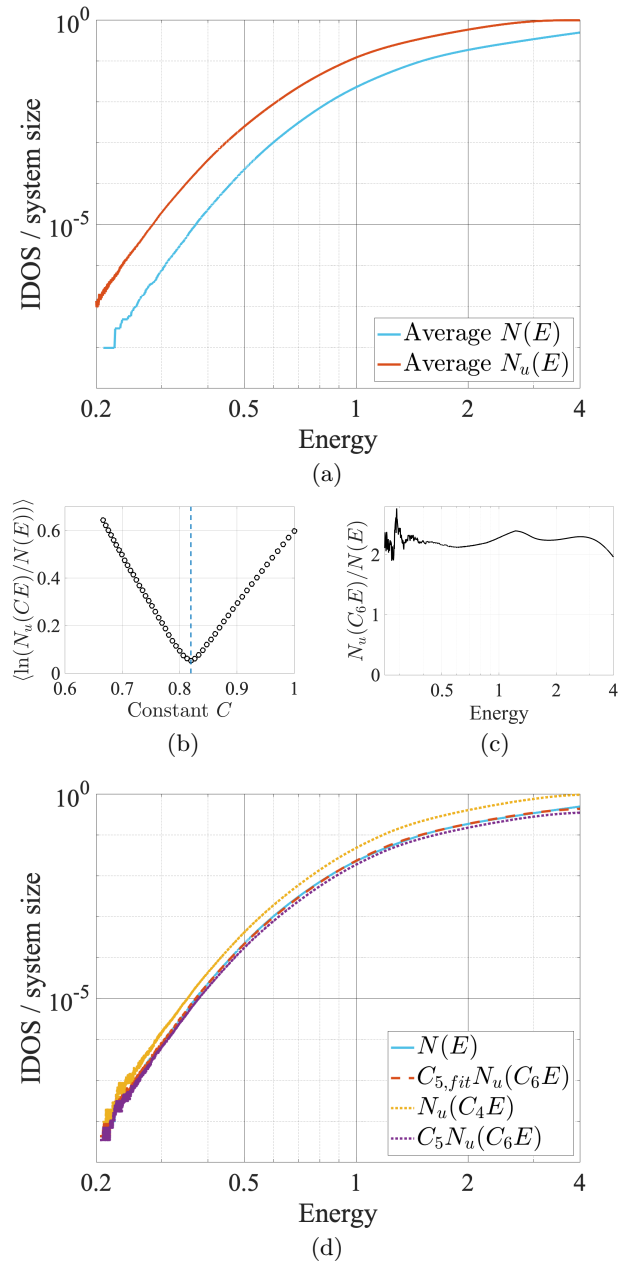


FIG. 4. (a)  $N(E)$  (blue) averaged over 1000 random realizations, and averaged landscape law  $N_u(E)$  (red), for a one-dimensional uniform Anderson tight-binding model of size  $N = 10^5$  and  $V_{\max} = 4$ . (b) Standard deviation of the distribution of values of  $\ln(N_u(CE)/N(E))$  for various values of  $C$ . The minimum around  $C = 0.82 \approx 1/1.22$  provides the value of  $C_6$ . (c) Plot of  $N_u(C_6 E)/N(E)$ . The maximum in the noiseless part of the graph shows that one can take  $C_5 = 1/2.77$ . A best fit for  $N(E)$  is obtained by taking the average value  $C_{5,\text{fit}} \approx 1/2.23$ . (d) Final comparison between the original  $N(E)$ , the best fit  $C_{5,\text{fit}} N_u(C_6 E)$ , and the two bounds from above of below  $N_u(C_4 E)$  and  $C_5 N_u(C_6 E)$  (dotted lines).

especially at larger energy. This reflects the fact that the prefactor of  $N_u(E)$  has to be different at low and at high

energy in order to approximate with precision  $N(E)$ .

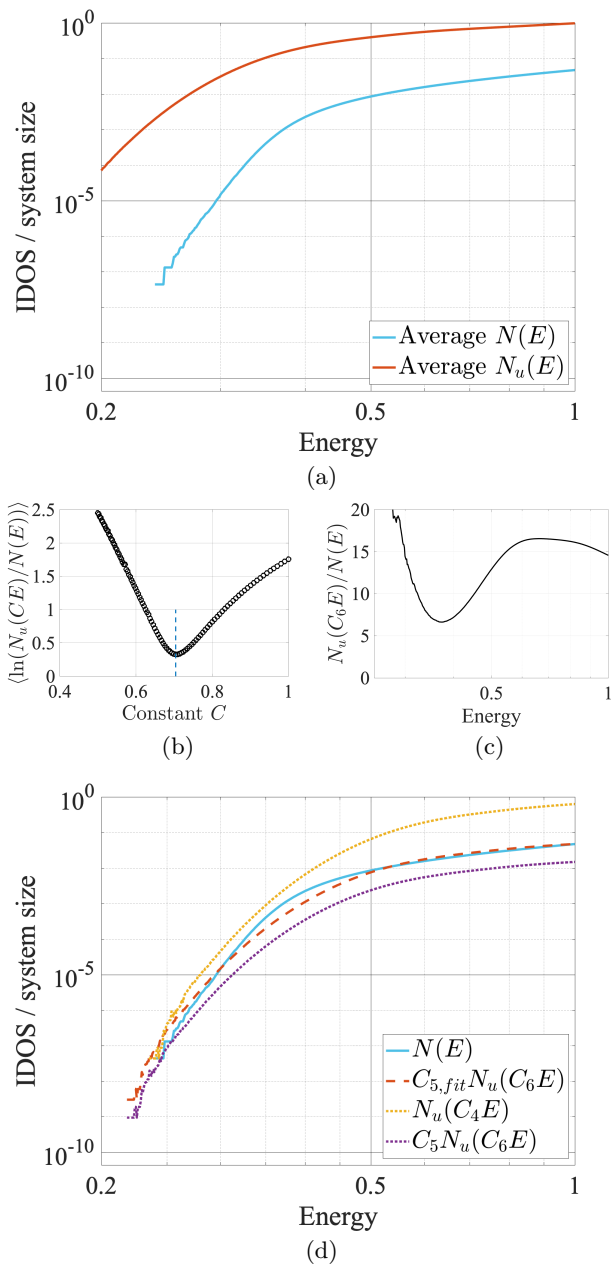


FIG. 5. (a)  $N(E)$  (blue) averaged over 100 random realizations, and averaged landscape law  $N_u(E)$  (red), for a two-dimensional binary Anderson tight-binding model of size  $N = (1500)^2$ . (b) Standard deviation of the distribution of values of  $\ln(N_u(CE)/N(E))$  for various values of  $C$ . The minimum around  $C = 0.7 \approx 1/1.42$  provides the value of  $C_6$ . (c) Plot of  $N_u(C_6 E)/N(E)$ . Its maximum for  $E > 0.3$  shows that one can take  $C_5 = 1/46.4$  which is also almost the best fit  $C_{5,fit} \approx 1/14.5$ . (d) Final comparison between the original  $N(E)$ , the best fit  $C_{5,fit} N_u(C_6 E)$ , and the two bounds from above of below  $N_u(C_4 E)$  and  $C_5 N_u(C_6 E)$  (dotted lines).

Table I summarizes the values obtained for the constants in all cases. This table triggers several comments.

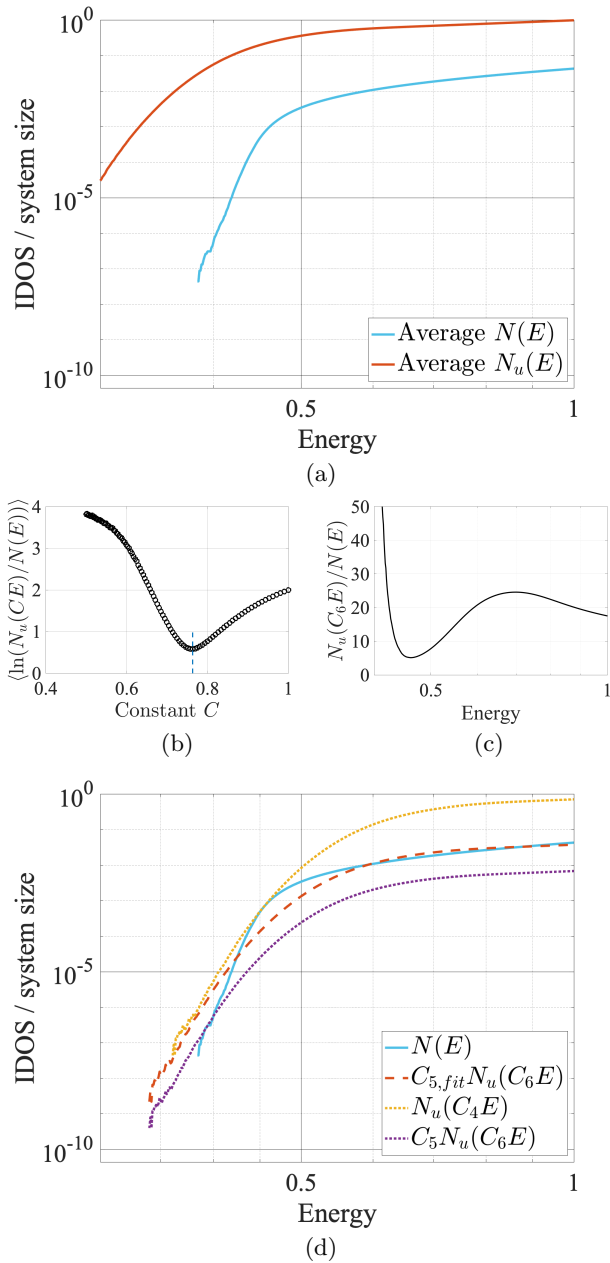


FIG. 6. (a)  $N(E)$  (blue) averaged over 100 random realizations, and averaged landscape law  $N_u(E)$  (red), for a two-dimensional uniform Anderson tight-binding model of size  $N = (1500)^2$ . (b) Standard deviation of the distribution of values of  $\ln(N_u(CE)/N(E))$  for various values of  $C$ . The minimum around  $C = 0.76 \approx 1/1.31$  provides the value of  $C_6$ . (c) Plot of  $N_u(C_6 E)/N(E)$ . Its maximum for  $E > 0.4$  shows that one can take  $C_5 = 1/111$  while the best fit leads to  $C_{5,fit} \approx 1/20.1$ . (d) Final comparison between the original  $N(E)$  (blue), the best fit  $C_{5,fit} N_u(C_6 E)$  (red), and the two bounds from above of below  $N_u(C_4 E)$  and  $C_5 N_u(C_6 E)$  (dotted lines).

First, the values of  $1/C_4$  are totally consistent with the value  $1 + d/4$ , where  $d$  is the ambient dimension. This value arises in the localization landscape approach as the

ratio between a local fundamental eigenvalue inside a localization region and the local minimum of the effective potential  $W = 1/u$  [24, 25]. From the definition of  $N_u(E)$ , at a given energy  $E$ , a  $d$ -cube of sidelength  $E^{-1/2}$  contributes to  $N_u(E)$  only if  $\min(W)$  inside the cube is smaller than  $E$ . In that situation, one would expect a local fundamental eigenvalue roughly at  $(1 + d/4)W_{\min}$ . Consequently, there is a natural multiplicative shift in energy between  $N(E)$  and  $N_u(E)$ , by a factor  $1 + d/4$ . This is what is found in our 1D and 2D simulations. One has to note that this shift has already been observed in a very different model, namely the “pieces model” in which a one-dimensional system is partitioned into sub-intervals of random length following a Poisson law [26, 27].

Secondly, the values of  $C_6$  follow also very closely that of  $C_4$ , only slightly smaller. We observe that the values of  $C_6$  are closer to that of  $C_4$  for Anderson uniform models.

Thirdly, the results displayed in Table I help us understand the influence of the disorder intensity  $V_{\max}$ . To that end, we have set  $V_{\max} = 1, 2$ , or  $4$  for Anderson binary and Anderson uniform models in 1D and 2D. The theory developed in [1] states that the constants involved in the bounds should not depend of the maximum value of the potential but on its average value. However, in both Anderson binary and Anderson uniform models, the average value of the potential is  $\langle V \rangle = V_{\max}/2$ , so it is still directly determined by the disorder intensity. In all computed cases, we observe that the values of  $C_4$  and  $C_6$  remain almost unchanged while the value of  $C_{5,\text{fit}}$  appears to be roughly proportional to  $V_{\max}^{1/2}$ , which is a natural scaling in the problem at hand.

Model	$L$	$V_{\max}$	$1/C_4$	$1/C_5$	$1/C_{5,\text{fit}}$	$1/C_6$		
1D	binary	1	1.26	5.45	4.08	1.11		
		$10^5$	2	1.3	3.78	3.03	1.2	
		4	1.26	2.91	2.04	1.32		
	uniform	$10^4$	1	1.27	8.18	4.15	1.1	
		$10^3$	1	1.26	5.96	4.27	1.08	
		1	1.28	4.85	3.94	1.19		
	2D	binary	$10^5$	2	1.24	8.14	3.36	1.19
			4	1.24	2.77	2.23	1.22	
			$10^4$	1	1.28	7.81	4.05	1.18
		uniform	$10^3$	1	1.27	8.86	4.29	1.16
1500			1	1.53	46.4	14.5	1.42	
2			1.54	33.8	9.00	1.44		

TABLE I. Summary of the values found for the constants  $C_4$ ,  $C_5$ ,  $C_{5,\text{fit}}$ , and  $C_6$ .  $L$  is the sidelength (so that the system size is  $|\Omega| = L^d$ ), and  $V_{\max}$  is the maximum value of the potential.

One can mention that an alternative way of relating  $N(E)$  and  $N_u(E)$  at the bottom of the spectrum, and therefore of extracting the constants involved in Eq. (6), consists in using a corollary of the Landscape Law pertaining to the scaling at low energies for all random i.i.d. potentials [1]. In this article, it is shown that, in the

case of an Anderson tight-binding model where the on-site potential values  $\{V_i\}$  follow a random law of cumulative distribution function  $F$  (i.e., the probability to have  $V_i \leq E$  is  $F(E)$ ), there exist constants  $\gamma_1, \gamma_2, \gamma_3, \gamma_4, c_1, c_2$  such that

$$\gamma_3 F(c_2 E)^{\gamma_4 E^{-\frac{d}{2}}} \leq \frac{N(E)}{E^{\frac{d}{2}}} \leq \gamma_1 F(c_1 E)^{\gamma_2 E^{-\frac{d}{2}}} \quad (7)$$

More specifically, in the case of binary and uniform random laws, one has  $F(E) = 1/2$  and  $F(E) = E$  for  $0 < E < 1$ , respectively. Therefore, with a slight change of the meaning of  $\gamma_4$ ,

$$\gamma_3 e^{\gamma_4 E^{-\frac{d}{2}}} \leq N(E) E^{-\frac{d}{2}} \leq \gamma_1 e^{\gamma_2 E^{-\frac{d}{2}}} \quad (8)$$

$$\gamma_3 e^{\gamma_4 E^{-\frac{d}{2}} |\ln(E)|} \leq N(E) E^{-\frac{d}{2}} \leq \gamma_1 e^{\gamma_2 E^{-\frac{d}{2}} |\ln(E)|} \quad (9)$$

Let us consider the binary Anderson model. The inequality (8) can be rewritten

$$\begin{aligned} \gamma_4 + \ln(\gamma_3) E^{\frac{d}{2}} &\leq E^{\frac{d}{2}} \ln \left( N(E) E^{-\frac{d}{2}} \right) \\ &\leq \gamma_2 + \ln(\gamma_1) E^{\frac{d}{2}} \end{aligned} \quad (10)$$

In other words, the quantity  $E^{\frac{d}{2}} \ln \left( N(E) E^{-\frac{d}{2}} \right)$  can be bounded between two affine functions of  $E^{\frac{d}{2}}$ . In the uniform Anderson model, a similar expression holds with only a logarithmic correction:

$$\begin{aligned} \gamma_4 + \ln(\gamma_3) \frac{E^{\frac{d}{2}}}{|\ln(E)|} &\leq \frac{E^{\frac{d}{2}}}{|\ln(E)|} \ln \left( N(E) E^{-\frac{d}{2}} \right) \\ &\leq \gamma_2 + \ln(\gamma_1) \frac{E^{\frac{d}{2}}}{|\ln(E)|} \end{aligned} \quad (11)$$

Figure 7 displays the graphs of these quantities near  $E = 0$  in three different cases already examined: (i) a 1D binary Anderson model (cf. Fig. 2), (ii) a 1D uniform Anderson model (cf. Fig. 3), and (iii) a 2D uniform Anderson model (cf. Fig. 6). In each case, the values of  $\gamma_1, \gamma_2, \gamma_3, \gamma_4$  are extracted from the scaling behavior of  $N(E)$  and  $N_u(E)$  (the linear scaling relations expressed in Eqs. (10) and (11) are shown in dotted lines in the graphs), and then used to compute the effective values of  $C_5$  and  $C_6$  relating  $N$  to  $N_u$ . The findings are grouped in Table II. One has to underline that the huge computation time required to reach very low values of  $E$  limits the accuracy and the range of the data on which the scaling could be efficiently be performed, and led to significant error bars. It precluded performing this analysis in the 2D uniform Anderson model. Even in the 2D binary Anderson model (Fig. 7c), the scaling is observed for a very limited range of energy. Yet, we observe in 1D (see Fig. 7a,b) the scaling predicted by the mathematical proof in [1]. The parameters  $C_5$  and  $C_6$  are consistent with the values reported in Table I, confirming that  $N_u$  can be used through Eq. (6) to approximate  $N(E)$  throughout the spectrum. Finally, in 2D (Fig. 7c), the

discrepancy in the values of  $C_5$  clearly indicates that one cannot find a single prefactor satisfying Eq. (6), and that this prefactor has in fact to be modified into a very slowly varying function from  $E = 0$  to the largest eigenvalue.

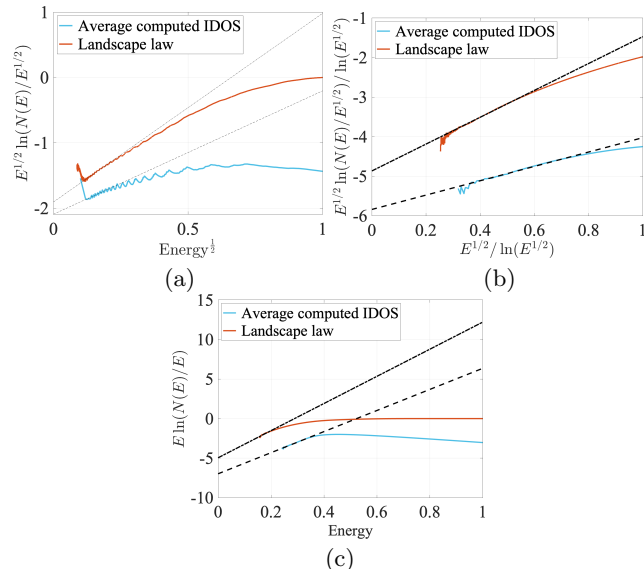


FIG. 7. Scaling behavior of  $N(E)$  and  $N_u(E)$  near  $E = 0$ . The straight lines correspond to the asymptotic linear behaviors appearing in Eqs. (10) and (11). (a) 1D binary Anderson model. (b) 1D uniform Anderson model. (c) 2D binary Anderson model.

Model	$V_{\max}$	$1/C_{5,\text{fit}}$	$1/C_6$	$1/C_5$	$1/C_6$
1D	binary	1	4.08	1.11	2.55
	uniform	1	3.95	1.19	4.05
2D	binary	1	14.5	1.42	0.84

TABLE II. Comparisons between the constants  $C_{5,\text{fit}}$  and  $C_6$  from Table I and the constants  $C_5$  and  $C_6$  obtained from the scaling analysis near  $E = 0$ .

Finally, the general picture that emerges from this exhaustive numerical study is that  $N_u(E)$  follows very closely the behavior of the actual IDOS  $N(E)$  throughout the entire energy range while being at the same time much easier to compute and to handle. Although it is not always possible to approximate  $N(E)$  through one single expression such as Eq. 6, one can wonder whether we could obtain a very good estimate with almost universal constants. First, we remind that the values found for the constant  $C_6$  are all very close to  $1/(1+d/4)$ , for a reason expressed in [25]. A natural universal approximation for  $N(E)$ , without any fitting parameter, could thus be proportional to  $N_u(E/(1+d/4))$ . To test this hypothesis, we plot the ratio  $N(E)/N_u(E/(1+d/4))$  vs.  $E$  for all cases reported in Table I, see Fig. 8.

We observe that in 1D, all curves for all tested potentials (binary or Anderson models, different values  $V_{\max}$ , different system sizes) follow the same pattern, i.e., a slow

evolution from a value close to 2 at low energy to a value close to 4 at larger energy. In 2D, the structure is similar with a wider dynamics, from about 1 to about 16. This means that while the IDOS  $N(E)$  spans several orders of magnitude (about 6 to 10 in our examples), the function  $N_u(E/(1+d/4))$  remains always remarkably close to  $N(E)$ . The prefactor appears to be different in the low and high energy regime, although it seems within reach, at least in 1D, to derive a very slowly varying function of the energy that would account for this change of prefactor. This change of prefactor between the low and the high energy regimes can be understood since one knows that, at least in the continuous setting,  $N(E)/N_u(E)$  is equivalent to  $\omega_d/(2\pi)^d$  at higher energy (so independent of the potential), with  $\omega_d$  the volume of the unit ball in dimension  $d$ : as soon as  $E > V_{\max}$ , all cubes satisfy the condition in Eq. (4) and  $N_u(E) = E^{d/2}$ . On the other hand, in the low energy limit, one expects  $N(E)$  to behave as  $N_u(E/(1+d/4))$  which implies a different prefactor depending on the type of potential.

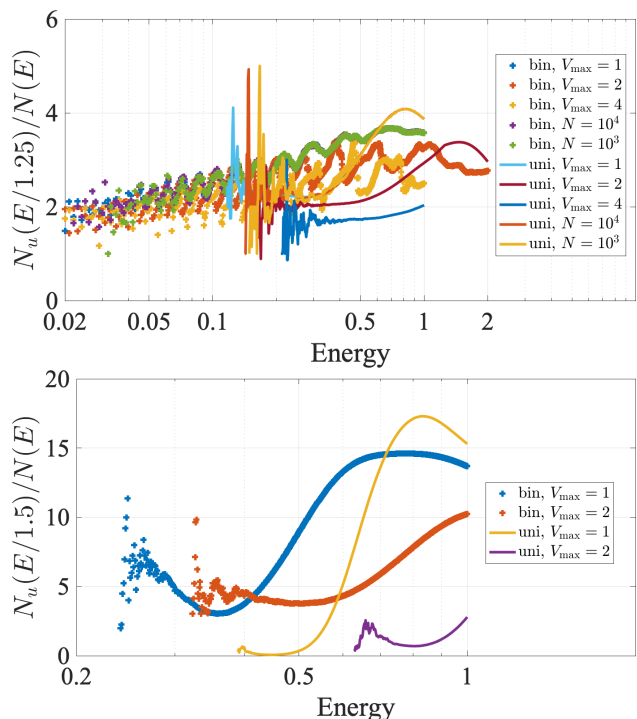


FIG. 8. Ratio  $N_u(E/(1+d/4))/N(E)$  plotted as a function of the energy  $E$ . (Top) For all 1D models reported in Table I. (Bottom) For all 2D models reported in Table I.

In conclusion, we have presented here a new function called the Landscape Law which provides for the first time bounds from above and below to the integrated density of states of quantum systems. Not only this Landscape Law, derived from the localization landscape, is remarkably faster to compute than the entire IDOS especially in random or disordered systems, but it also captures the scaling behavior of Anderson models near the bottom of the spectrum to an unprecedented precision,

even accounting for a logarithmic correction between the binary and uniform Anderson models. In one dimension, the bounds are so close that in fact, one single formula approximates the IDOS throughout the entire spectrum, with only a prefactor  $C_5$  and a multiplicative shift  $C_6$  on the energy consistent with the “ $(1 + d/4)$ ” formula found in [25]. In two dimensions, the bounds still provide a satisfactory approximation to the IDOS, but they cannot be merged into one single formula. One needs to modify the prefactor between the bottom and the top of the spectrum. In summary, the Landscape Law therefore promises to be a remarkable tool for investigating

the properties of IDOS in many random or disordered potentials, not only theoretically but also numerically. In particular, it opens the perspective of assessing accurately the density of states in systems of very large sizes without having to compute one eigenvalue.

## ACKNOWLEDGMENTS

This work was supported by grants to several of the authors from the Simons Foundation (601937, DNA; 601941, GD; 601944, MF; 563916, SM) and, in part, by the DMS NSF 1839077.

- 
- [1] G. David, M. Filoche, and S. Mayboroda, “The landscape law for the integrated density of states,” (2019), arXiv:1909.10558 [math.AP].
- [2] I. M. Lifshitz, Adv. Phys. **13**, 483 (1964).
- [3] I. M. Lifshitz, Soviet Physics Usp **7**, 549 (1965).
- [4] L. Pastur and A. Figotin, *Spectra of Random and Almost-Periodic Operators*, Grundlehren der Mathematischen Wissenschaften (Springer, 1992).
- [5] W. Kirsch and B. Metzger, in: F. Gesztesy, P. Deift, C. Galvez, P. Perry, W. Schlag (Editors): Spectral Theory and Mathematical Physics: A Festschrift in Honor of Barry Simon’s 60th Birthday. , 649 (2007).
- [6] W. König, *The Parabolic Anderson Model, Random Walk in Random Potential*, Pathways in Mathematics (Springer, 2016).
- [7] M. Benderskii and L. Pastur, Mathematics of the USSR-Sbornik **11**, 245 (1970).
- [8] M. D. Donsker and S. S. Varadhan, Commun. Pure Appl. Math. **28**, 525 (1975).
- [9] S. Nakao, Japan. J. Math. New series **3**, 111 (1977).
- [10] L. Pastur, Theoret. Math. Phys. **32**, 615 (1977).
- [11] W. Kirsch and F. Martinelli, Commun. Math. Phys. **89**, 27 (1983).
- [12] B. Simon, J. Stat. Phys. **38**, 65 (1985).
- [13] G. Mezincescu, Commun. Math. Phys. **103**, 167 (1986).
- [14] M. Biskup and W. König, Ann. Probab. **29**, 636 (2001).
- [15] F. Klopp, Commun. Math. Phys. **232**, 125 (2002).
- [16] F. Klopp, Ann. Henri Poincaré **3**, 711 (2002).
- [17] A. Elgart *et al.*, Duke Math. J. **146**, 331 (2009).
- [18] J. M. Luck and T. M. Nieuwenhuizen, J. Stat. Phys. **52**, 1 (1988).
- [19] A. Politi and T. Schneider, Europhysics Letters (EPL) **5**, 715 (1988).
- [20] M. Filoche and S. Mayboroda, Proc. Natl Acad. Sci. USA **109**, 14761 (2012).
- [21] D. N. Arnold, G. David, D. Jerison, S. Mayboroda, and M. Filoche, Phys. Rev. Lett. **116**, 056602 (2016).
- [22] M. L. Lyra, S. Mayboroda, and M. Filoche, EPL (Europhysics Letters) **109**, 47001 (2015).
- [23] B. N. Parlett, *The Symmetric Eigenvalue Problem* (Society for Industrial and Applied Mathematics, 1998) <https://locus.siam.org/doi/pdf/10.1137/1.9781611971163>.
- [24] D. N. Arnold, G. David, M. Filoche, D. Jerison, and S. Mayboroda, Commun. Part. Diff. Eq. **44**, 1186 (2019).
- [25] D. N. Arnold, G. David, M. Filoche, D. Jerison, and S. Mayboroda, SIAM J. Sci. Comput. **41**, B69 (2019).
- [26] A. Comtet and C. Texier, Phys. Rev. Lett. **124**, 219701 (2020).
- [27] M. Filoche, D. Arnold, G. David, D. Jerison, and S. Mayboroda, Phys. Rev. Lett. **124**, 219702 (2020).